International Journal of Science and Research (IJSR)
ISSN (Online): 2319-7064
Index Copernicus Value (2015): 78.96 | Impact Factor (2015): 6.391

Analyses of Quantum Chemical Parameters, Fukui Functions, Magnetic Susceptibility, Hyperpolarizability, Frontier Molecular Orbitals, NBO, Vibrational and NMR Studies of 1(4-Aminophenyl) Ethanone

M. Karunanidhi[1], V. Balachandran[2], B. Narayana[3], M. Karnan[4]

[1, 4]Department of Physics, Srimad Andavan Arts and Science College (Autonomous), Tiruchirappalli 620005, India

[2]Centre for Research, Department of Physics, A.A. Government Arts College, Musiri 621211, India

[3]Department of Studies in Chemistry, Mangalore University, Mangalagangotri 574 199, India

Abstract: ***Various quantum chemical parameters such as ionization potential, electron affinity, chemical hardness, electro negativity, local softness, chemical potential and the appropriate local quantities of 1(4-Aminophenyl)ethanone (APE) have been calculated. The entire quantum chemical calculations and optimized structural parameters (bond lengths and bond angles), vibrational frequencies and optimized geometry have performed at DFT/B3LYP method with cc-pVDZ and cc-pVTZ basis sets using the Gaussian 09W program package. The FTIR and FT Raman spectra of 1(4-Aminophenyl)ethanone have been recorded in the regions 4000 – 400 cm $^{-1}$ and 3500 – 100 cm^{-1}, respectively. The calculated harmonic vibrational frequencies have been compared with experimental FTIR and FT Raman spectra. The observed and calculated frequencies are found to be in good agreement. The effects of substituent (amino and acetyl groups) on the benzene ring vibrational frequencies are analyzed. ^{1}H and ^{13}C NMR isotropic chemical shifts are calculated and assignments made are compared with the experimental values. Magnetic susceptibility and thermodynamic properties have been determined for various range of temperature. The energies of frontier molecular orbitals, hyperpolarizability, total electron density and electrostatic potential of the title compound are determined. Mulliken analysis on atomic charges, local reactivity descriptors such as local softness (s_k),Fukui function(f_k), global electrophilicity and nucleophilicity of the title compound have also been calculated.***

Keywords: Quantum chemical parameters, Magnetic susceptibility, Fukui function, 1(4-Aminophenyl) ethanone, Hyperpolarizability, Thermodynamic properties

1. Introduction

Acetophenone occurs naturally in many foods including apple, cheese, apricot, banana and cauliflower. Commercially significant resins of acetophenone with formaldehyde and base resulting polymers are used as components of coatings, adhesives and inks. Acetophenone is used to create fragrances that correspond to almond, cherry, honeysuckle, jasmine and strawberry. It is used in medicine; it was marketed as a hyptonic and anticonvulsant under the brand name hypnone. Chloro acetophenone is primarily used as a riot-control agent (tear gas) and in Chemical Mace [1,2]. Hydroxyacetophenone is used as a building block for the synthesis of rubbers, plastics, pharmaceuticals, agrochemicals, flavor and fragrances. In pharmaceuticals hydroxyacetophenone is employed as an intermediate for the synthesis of medicine named as propafenone which is used for curing arrhythmia [3]. Recent studies revealed that studies of aminophenylacetophenone and their complexes have received most of attention, because of magnetic, spectroscopic, biological and photosensitive properties. Aminophenylacetophenone have shown a wide variety of anticancer, antimicrobial, antifungal, antidepressant antitumor, antibacterial, anti-inflammatory and anticonvulsant activities [4].

The vibrational analyses of this molecule would be helpful for understanding the various types of bonding and normal modes of vibration. In recent trends, the quantum chemical computational methods have proved to be an essential tool in analyzing the vibrational spectra. Subramanian et al.[5], have extensively studied the thermodynamic properties of 3-aminoacetophenone. Seth et al. [6] investigated the spectroscopic and X-ray structure of ortho-hydroxy acetophenones. Pei et al. [7] investigated the Franck–Condon region photodissociation dynamics of p-nitroacetophenone using resonance Raman spectroscopy and density functional theory calculations. Literature survey reveals that to the best of our knowledge no DFT/B3LYP method with cc-pVDZ and cc-pVTZ basis sets and magnetic susceptibility, fukui function, thermodynamic calculations, and experimental (FT-IR, FT-Raman and NMR) investigation of APE are reported so far. Therefore, an attempt has been made in the present work to study the detailed theoretical DFT/B3LYP method with cc-pVDZ and cc-pVTZ basis sets and magnetic susceptibility, fukui function, thermodynamic properties, and experimental (FTIR and FT Raman, ^{1}H and ^{13}C NMR) spectral investigation of APE.

2. Experimental Details

The sample APE in the solid form was purchased from the Lancaster Chemical Company, (UK) with a purity of greater than 97% and it was used as such without further purification. The Fourier transform infrared (FT-IR) spectrum of the sample was recorded at room temperature in the region 4000–400 cm^{-1} using Perkin–Elmer spectrum RX1 spectrophotometer equipped with composition of the pellet.The signals were collected for 100 scans with a scan interval of $1cm^{-1}$ and at optical resolution of 0.4 cm^{-1}.The Fourier transform Raman (FT-Raman) BRUKER-RFS 27 spectrometer was used for the Raman spectral measurements at room temperature. The spectrometer consisted of a quartz beam splitter and a high sensitive germanium diode detector cooled to the liquid nitrogen temperature. The sample was packed in a glass tube of about 5 mm diameter and excited in the 180° geometry with 1064 nm laser line at 100mW power from a diode pumped air cooled-cw Nd:YAG laser as an excitation wavelength in the region 4000–100 cm^{-1}. The signals were collected for 300 scans at the interval of $1cm^{-1}$ and optical resolution of 0.1 cm^{-1}.

2.1 NMR spectroscopy

Nuclear magnetic resonance (NMR) spectra were recorded on a Bruker 300 AVANCE spectrometer at 300 MHz for ^{1}H and 75 MHz for ^{13}C in CDCl3 solutions containing 0.03 vol.% TMS as internal standard.

2.2. Methods of computation

The entire quantum chemical calculations have performed at DFT/B3LYP method with cc-pVDZ and cc-pVTZ basis sets using the Gaussian 09W program package [8]. The optimized structural parameters have been evaluated for the calculation of vibrational frequencies at Becke's three parameter hybrid model using the Lee–Yang–Parr [9,10] correlation functional (B3LYP) method. As a result, the unscaled calculated frequencies, infrared intensity, Raman activity, are obtained. In order to fit the theoretical frequencies to the experimental frequencies, an overall scaling factor has been introduced by using a least-square optimization. The vibrational frequencies are scaled as 0.9899 for frequencies less than 1700 cm^{-1} and 0.9552 for higher frequencies for B3LYP. After scaled with the scaling factor, the deviation from the experiments is less than 10 cm^{-1} with a few exceptions. The assignments of the calculated normal modes have been made on the basis of the corresponding PEDs. The PEDs are computed from quantum chemically calculated vibrational frequencies using MOLVIB program version 7.0 written by Sundius [11, 12]. Gauss view program [13] has been considered to get visual animation and also for the verification of the normal modes assignment.

2.3. Prediction of Raman intensities

The Raman activities (S_i) calculated with the help of GAUSSIAN 09 program were converted to relative Raman intensities (I_i) using the following relationship derived from the basic theory of Raman scattering [14–16]. $I_i = f(\nu_0-\nu_i)^4 S_i / \nu_i[1-\exp(-hc\nu_i/kt)]$ where ν_0 is the laser exciting frequency in cm^{-1} (in this work, we have used the excitation wave number ν_0 = 9398.5 cm^{-1}, which corresponds to the wavelength of 1064 nm of a Nd:YAG laser), ν_i is the vibrational wave number of the i^{th} normal mode(in cm^{-1}) and S_i is the Raman scattering activity of the normal mode ν_i, f (is the constant equal to 10^{-12}) is the suitably chosen common normalization factor for all peak intensities. h, k, c, and T are Planck constant, Boltzmann constant, speed of light and temperature in Kelvin, respectively.

3. Structural properties

The optimized stable geometry and the scheme of atom numbering of the compound APE are represented in Fig.1. The optimized structural parameters bond length, bond angle and the dihedral angle for the more stable geometry of APE determined at B3LYP with cc-pVDZ and cc-pVTZ basis sets are presented in Table 1. The influence of the substituent on the molecular parameters, particularly in the C-C bond distance of ring carbon atoms seems to be varied. The mean bond length of aromatic ring is 1.40 Å. The longer bond length (1.48 Å) of C1-C7 is due to the absence of delocalization of carbonyl lone pair of electrons towards the ring. Similarly, the bond C7-C9 has 1.52 Å because of the hyper conjugative effect of the methyl group and due to the partial ionic character of the C-O group, decreases in force constant and increase in bond length. The bond length of C7-O8 and C7-C9 are 1.22 and 1.52 Å, respectively shows an excellent results with the bond length of 4-hydroxy 3-methoxyacetophenone [17]. While the bond length C7-O8 (1.22 Å) of 2H4MAP is elongated with respect to acetophenone (C-O; 1.216Å) [18]. But in the case APE the orientations of the carbonyl, methyl and amino groups with respect to the aromatic ring are perfectly planar. This is confirmed by the dihedral angle, C7-C1-C2-C3; -180°, C7-C1-C6-C5; 180°, C6-C1-C7-C9; 180°, C2-C1-C7-C9; 0°, C2-C3-C4-N15; -180°, N15-C4-C5-C6; 180°. Analyzing the bond angle of aromatic ring of APE, one can observe that the geometry of the benzene ring is seen to be relatively perturbed due to the presence of different substituent's. With the electron donating and withdrawing substituent's on the benzene ring, the symmetry of the ring is distorted, yielding variation in bond angles at the point of substitution and at the ortho and meta positions as well. The studies indicated that the interior bond angle, at the carbon to which a methyl or amino group is attached, is invariably smaller than that normally adopted as the interior bond angle of the benzene ring [19, 20]. On the other hand, the interior bond angle at the carbon to which a nitro group is attached invariably exceeds the normal 120° [21]. The bond angle C2-C1-C6 is 117.7° where the $-COCH_3$ group is attached while at ortho positions the bond angle C1-C2-C3 is found to be 121.3° while the bond angle C1-C6-C5 is 121.5°. This indicates that the inner bond angle is less than 120° where the electron withdrawing acetyl group attached while the inner ortho bond angles are more than 120°. This is also due to the predominance of the partial ionic nature of the carbonyl group. Similarly, the bond angle C3-C4-C5 where the amino group attached is 118.2°, 118.4°. These are determined by B3LYP/ cc-pVDZ and cc-pVTZ method.

4. Vibrational Analysis

The geometry of the molecule is possessing Cs point group symmetry. The 51 fundamental modes of vibrations are span into 35 in-plane modes of A' and 16 out-of-plane bending vibrations of A" species. The observed and calculated FTIR and FT-Raman spectra of APE are shown in Figs. 2 and 3. The observed FTIR and FT-Raman wavenumbers along with the theoretical IR and Raman frequencies along with their relative intensities and probable assignments are summarized in Table 2.

4.1 Skeletal stretching vibrations

The carbon–carbon vibrations are more interesting if the double bond is in conjugation with the ring. The actual positions of the C-C stretching modes are determined not so much by the nature of substituent but by the form of the substitution around the ring [22, 23]. The C-C bands which indicate aromatic properties of benzene derivatives mainly occur within the range of 1640– 1200 cm^{-1}. The strong bands observed in the infrared spectrum at 1565, 1360 cm^{-1} and in Raman spectrum the medium lines observed at 1612, 1564 cm^{-1} are assigned to the C-C stretching modes of APE. The modes observed at 960, 958, 823, 733, 636, 564, 560, 469, 335 cm^{-1} in infrared and Raman spectra are assigned to the C-C-C in-plane ring trigonal bending vibration. The other in-plane bending vibrations are assigned to the modes at 574, 456 and 417 cm^{-1}. The C-C-C out-of-plane bending modes are attributed to the low Raman frequencies [24].

4.2 C-H vibrations

The aromatic C-H stretching vibrations are normally found between 3100 and 3000 cm^{-1} [25]. In this region the bands are not affected appreciably by the nature of substituent. The aromatic C-H stretching vibrations present in the benzene ring of APE are seen in the infrared spectrum as medium bands at 3086 and 3063 cm^{-1} and in Raman spectrum the medium lines observed at 3065, 3046 and 3025 cm^{-1}.The aromatic C-H in-plane bending modes of benzene and its derivatives are observed in the region 1300–1000 cm^{-1}. The peaks seen at 1514, 1437, 1173 and 1134 cm^{-1} in IR spectrum and 1516, 1441, 1171 cm^{-1} in Raman spectrum belongs to the aromatic C-H in-plane bending vibrations. The C-H out-of-plane bending mode of benzene derivatives are observed in the region 1100–600 cm^{-1}. The aromatic C-H out-of-plane bending vibrations of APE are seen in the Raman spectrum at 943, 901, 811 and 785 cm^{-1}.

4.3. Methyl group vibrations

The methyl substituted C–H stretching vibrations usually appears below the range of aromatic C–H stretching. Methyl group vibrations are generally referred to as electron donating substituent in the aromatic rings system, the asymmetric C-H stretching mode of CH_3 is expected around 2980 cm^{-1} and the CH_3 asymmetric stretching is expected at 2870 cm^{-1} [26,27]. The weak bands observed in the infrared spectrum at 2842, 2819 cm^{-1} and in Raman spectrum the weak line observed at 2975 cm^{-1} are assigned to the CH_3 stretching modes of APE. The theoretically calculated values by B3LYP/cc-pVDZ method at 2975, 2843, 2824cm^{-1} and B3LYP/cc-pVTZ method at 2973, 2840, 2820 cm^{-1} are coherent with the literature data. The asymmetric and symmetric deformation vibrations of methyl group appear within the region 1465–1440 cm^{-1} and 1390–1370cm^{-1} [26]. In the present investigation, the bands at 1304cm^{-1} in infrared with medium intensity 1386, 1375 and 1305 cm^{-1} in Raman with strong intensity are observed as CH_3 asymmetric deformation and symmetric deformation vibrations. The theoretically calculated values by B3LYP/cc-pVDZ method at 1389,1378 and 1312 cm^{-1} shows good agreement with experimental values. The methyl rocking mode vibration usually appears within the region 1070–1010cm^{-1} [27]. With reference to literature data, a band observed at 1073, 1035cm^{-1} in Raman spectrum and 1073, 1035 cm^{-1} in FT-IR are assigned CH_3 rocking vibration. The DFT calculation gives rocking vibration at 1079 and 1038 cm^{-1} and 1074, 1029 cm^{-1} are quiet fit with experimental values. Torsional modes of vibrations are observed at very low frequencies. The computed frequency at 161, 145 cm^{-1} are assigned to torsional mode of vibration.

4.4. C=O vibrations

The characteristic infrared absorption frequency of C=O in acids are normally strong in intensity and found in the region 1800–1690 cm^{-1} [28]. This position of C=O stretching more effective to analyze the various factors in ring aromatic compounds. The C=O bond formed by = bond between C and O intermolecular hydrogen bonding, reduces the frequencies of the C=O stretching absorption to a greater degree than does intermolecular H bonding because of the different electro-negativities of C and O, the bonding are not equally distributed between the two atoms. The loan pair of electrons on oxygen also determines the nature of the carbonyl groups. The C=O stretching bands of acids are considerably more intense than ketonic C=O stretching bands. In the present study the characteristic ketonic C=O frequency appears at 1647 cm^{-1} in FT-IR and 1650 cm^{-1} in FT-Raman spectrum are assigned to C=O stretching vibration. The calculated values of 1659 and 1653 cm^{-1} at B3LYP/cc-pVDZ and B3LYP/cc-pVTZ levels of theory are in good agreement with the experimental value of C=O stretching mode. This C=O vibration appears in the expected range shows that it is not much affected by other vibrations. Kolev[29] showed that in aromatic and aliphatic ketones, the C=O in-plane and out-of-plane deformation modes are seen in 605–552 cm^{-1} and 584–285 cm^{-1} region, respectively. In the present study C=O in-plane bending vibration for APE is observed in FT-IR spectrum at 697 cm^{-1} and in FT-Raman spectrum at 689 cm^{-1}. The theoretically calculated values by B3LYP/cc-pVDZ and B3LYP/cc-pVTZ methods are 706 and 695 cm^{-1} shows good agreement with experimental values and also the theoretically calculated values of C=O out-of-plane bending vibration by DFT method at 605, 591 cm^{-1} are coherent with experimental value 596 cm^{-1} in FT-IR spectrum.

4.5. Amino group vibrations

According to Socrates [30] the frequencies of amino group appear around 3500–3300 cm^{-1} for NH_2 stretching, 1700–1600 cm^{-1} for scissoring and 1150–900 cm^{-1} for rocking deformations. For APE the antisymmetric and symmetric

stretching modes of NH_2 group were found at 3395, 3329 and 3325 cm^{-1} in infrared and Raman bands. The theoretically calculated values by B3LYP/cc-pVDZ and B3LYP/cc-pVTZ methods are 3398, 3341, 3394 and 3330 cm^{-1} shows good agreement with experimental values. The bands appeared at 1594 cm^{-1} in Raman spectrum was assigned to the scissoring mode of NH_2 group. The NH_2 rocking mode has been assigned in Raman band at 1003 cm^{-1} for the title compound (APE). The calculated values appear at 1604, 1593 cm^{-1} by cc-pVDZ and cc-pVTZ respectivly are assigned to scissoring mode and 1009, 1004 cm^{-1} are assigned to rocking mode of vibration are also good agreement with experimental frequencies. NH_2 twisting modes of APE are identified at 388cm^{-1}in Raman band and the calculated values appear at 401, 388 cm^{-1} by cc-pVDZ and cc-pVTZ respectivly are also good agreement with experimental frequencies.

5. Analysis of molecular electrostatic potential

Molecular electrostatic potential (MEP) mapping is very useful in the investigation of the molecular structure with its physiochemical property relationships [31-34]. Total SCF electron density surface mapped with molecular electrostatic potential (MEP) of APE determined by B3LYP/ cc-pVDZ is shown in Fig.4(a) while the contour map of the molecular electrostatic potential is given in Fig. 4(b). The MEP surface displays the molecular shape, size and electrostatic potential values. The colour scheme for the MEP surface is red-electron rich or partially negative charge; blue-electron deficient or partially positive charge; light blue-slightly electron deficient region; yellow-slightly electron rich region, respectively. The oxygen atoms have more negative potentials and the hydrogen atoms have more positive potentials. The MEP of APE clearly indicates the electron rich centre of oxygen atoms. The molecular electrostatic potential surface of APE determined by B3LYP/ cc-pVDZ method is shown in the Fig. 4(a). The minimum and maximum limits of the electrostatic potential observed in APE are $\pm 5.628e^{-10-2}$.

6. Natural bond orbital (NBO) analysis

Natural bond orbital (NBO) analysis is a useful tool for understanding delocalization of electron density from occupied Lewis-type (donor) NBOs to properly unoccupied non-Lewis type (acceptor) NBOs within the molecule. The stabilization of orbital interaction is proportional to the energy difference between interacting orbital. Therefore, the interaction having strongest stabilization takes place between effective donors and effective acceptors. This bonding, anti bonding interaction can be quantitatively described in terms of the NBO approach that is expressed by means of second-order perturbation interaction energy E(2) [35–38]. This energy represents the estimate of the off-diagonal NBO Fock matrix element. The stabilization energy $E^{(2)}$ associated with i (donor)→ j (acceptor) delocalization is estimated from the second-order perturbation approach as given below $E^{(2)} = q_i F^{(2)} (I,j)/\varepsilon_j-\varepsilon_i$ where q_i is the donor orbital occupancy, ε_i and ε_j are diagonal elements (orbital energies) and F(i, j) is the off-diagonal Fock matrix element. The different types of donor–acceptor interactions and their stabilization energy are determined by second order perturbation analysis of Fock matrix of APE. The stabilization energy of all lone pair–bond pair interactions and only bond pair–bond pair interactions are listed in Table 3. In APE molecule, the lone pair donor orbital, $n_N \rightarrow \pi^*_{cc}$ interaction between the (N15) lone pair and the C4 antibonding orbital gives a strong stabilization of 28.59kcal mol^{-1}. The $n_O \rightarrow \pi^*_{cc}$ to the antibonding orbital (π^*) of (C7) is 19.28kcal mol^{-1}. The bond pair donor → π^*stabilization energy of lone pair of electrons present in the oxygen atom orbital, $\pi_N \rightarrow \pi^*_C$ interactions give more stabilization than $\pi_O \rightarrow \pi^*_c$ and $\sigma_{cc} \rightarrow \sigma^*_{cc}$ interactions.The analysis of the natural bond orbital of APE by DFT/B3LYP method with cc-pVDZ and cc-pVTZ basis sets is carried out to provide the occupancy, contribution to the parent NBO and mainly on the percentage contributions of the atoms present in the bond. NBO analysis of molecules illustrate the deciphering of the molecular wave function in terms Lewis structures, charge, bond order, bond type, hybridization, resonance, donor–acceptor interactions, charge transfer and resonance possibility. Table.4. shows the accumulation of natural charges and electron population of atoms in core, valance, Rydberg orbitals of 1(4-Aminophenyl)ethanone. Table.5. depicts the bonding concepts such as type of bond orbital, their occupancies, the natural atomic hybrids of which the NBO is composed, giving the percentage of the NBO on each hybrid, the atom label and a hybrid label showing the hybrid orbital (sp_x) composition (the amount of s-character, p-character, etc.) of 1(4-Aminophenyl)ethanone determined by DFT/B3LYP method with cc-pVDZ and cc-pVTZ basis sets. The occupancies of NBO's reflecting their exquisite dependence on the chemical environment. The Lewis structure that is closest to the optimized structure is determined. For example, the bonding orbital for C1-C2 with 1.9735 electrons has 50.41% C1 character in a $sp^{1.85}$ hybrid and has 49.59% C2 character in a $sp^{1.82}$ hybrid orbital. In the case of C7-O8 bonding orbital with 1.996 electrons has 33.01% C7 character in a $sp^{2.28}$ hybrid and has 66.99% O8 character in a $sp^{1.30}$ hybrid orbital. A bonding orbital for C4-N15 with 1.990 electrons has 39.34% C4 character in a $sp^{2.93}$ hybrid and has 60.66% N15 character in a $sp^{1.62}$ orbital. The C-C bonds of the aromatic ring posses more p character than s character. This is clearly indicates the delocalization of p electrons among all the carbon atoms. For the title compound the dipole moment; linear polarizability and first hyperpolarizability were obtained from molecular polarizabilities based on theoretical calculations are listed in Table 6.

7. Mullikan Atomic Charges

Mullikan [38] atomic charge calculation has an important role for the application quantum chemical calculations (QCC) of the molecular system. Atomic charge affects dipole moment, polarizability, electronic structure and other molecular properties of the system. The calculated Mullikan charge (e) values of APE are listed in Table 7. It is clearly shown that the carbon atom attached with hydrogen atom is negative whereas the remaining carbon atoms are positively charged in the title compound. The oxygen and nitrogen atoms have more negative charges whereas all the hydrogen atoms have the positive charges. The more positive charge

of carbon is found for the title compounds are C2, C4, C6 and C7; it is mainly due to the substitution of negative charge of oxygen and nitrogen atoms. Illustration of atomic charge plotted for B3LYP/ cc-pVDZ and cc-pVTZ levels have been shown in Fig.5.

8. Frontier Molecular Orbital's Analysis

Highest Occupied Molecular Orbital (HOMO) and Lowest Unoccupied Molecular Orbital (LUMO) are very important parameters for quantum chemistry. The energies of HOMO, LUMO and their orbital energies are calculated using B3LYP/ cc-pVDZ and cc-pVTZ method and the pictorial illustration of the frontier molecular orbitals are shown in Fig. 6. Molecular orbitals provide insight into the nature of reactivity and some of the structural and physical properties of molecules. The positive and negative phase is represented in red and green colour, respectively. The plots reveal that the region of HOMO spread over the entire molecule of APE while in the case of LUMO it is spread over the entire molecule except on acetyl group. The calculated energy gap of HOMO–LUMO's explains the ultimate charge transfer interface within the molecule. The frontier orbital energy gap (LUMO-HOMO) is calculated by B3LYP/ cc-pVDZ and cc-pVTZ method, in case of APE is found to be 4.7515, 4.7589 eV.

9. Quantum Chemical Parameters

The quantum chemical parameters are predicted with the HOMO and LUMO orbital energy. Associated within the framework of SCF MO theory, the ionization energy and electron affinity can be expressed through HOMO and LUMO orbital energies as $I = -E_{HOMO}$ and $A = -E_{LUMO}$. The hardness corresponds to the gap between the HOMO and LUMO orbital energies .The larger the HOMO-LUMO energy gaps the harder the molecule. The global hardness is predicted using the relation $\eta = ½(E_{LUMO}-E_{HOMO})$. The hardness has been associated with the stability of chemical system. The reciprocal of the hardness will give the softness $\sigma = (1/\eta)$ of chemical system. The electron affinity can be used in combination with ionization energy to give electronic chemical potential, $\mu = 1/2(E_{LUMO}+E_{HOMO})$.The global electrophilicity index is $\omega = \mu^2/2\eta$ also calculated and presented in Table 8.

10. Magnetic Susceptibility

Atoms, molecules, free radicals or ions which contain one or more unpaired electron will possess permanent magnetic dipole moment that arises from the residual spin and angular moment of the unpaired electrons. All substances having permanent magnetic moment display paramagnetic behavior in nature. When a paramagnetic substance is placed in a magnetic field, they will align themselves in the direction of the field and thus produces positive magnetic susceptibility, which depends on the temperature; since thermal agitation will oppose the alignment of the magnetic dipoles. The effectiveness of diminishes increases with increase in temperature. The magnetic susceptibility (χ_m) of the molecules for various temperatures are predicted with knowledge of unpaired electron [39] and presented in Table 9. The graphical representation of ($1/\chi_m$) with T (temperature) is shown in Fig 7. The effective magnetic moment is found to be a constant, which is 5.92×10^{-6}(BM) and Curie constant is obtained from the magnetic moment (μ_m) and is found to be 0.00083.

11. NMR spectral studies

NMR spectroscopy has proved to be an exceptional tool to elucidate structure and molecular conformation. Density functional theory (DFT) shielding calculations are rapid and applicable to large systems. The ''gauge independent atomic orbital'' (GIAO) method [40–43] has proven to be quite accepted and accurate. To provide an explicit assignment and analysis of ^{13}C and ^{1}H NMR spectra, theoretical calculations on chemical shift of the title compound are carried out by GIAO method at B3LYP/ cc-pVDZ and cc-pVTZ level [44] with CDCl3 solvent. The ^{1}H and ^{13}C theoretical and experimental chemical shifts, isotropic shielding tensors and the chemical shift assignments are presented in Table 10. The hydrogen atoms are mostly localized on periphery of the molecules and their chemical shifts would be more susceptible to intermolecular interactions as compared to that for other heavier atoms. Unsaturated carbons give signals in overlapped areas of the spectrum with chemical shift values from 100 to 200 ppm [45]. ^{13}C NMR spectra exhibit signals somewhat downfield of 200 ppm depending on the structure. Such signals are typically weak due to the absence of nuclear Overhauser effects. The external magnetic field experienced by the carbon nuclei is affected by the electronegativity of the atoms attached to them. The effect of this is that the chemical shift of the carbon increases if the carbon is attached to an Thus, the carbonyl carbon atom C7 in APE show very downfield effect and the corresponding observed chemical shift is 195.55 ppm. The more electronegative character of the oxygen atoms renders a positive charge to the carbon and thus C1 chemical shift is observed in the more downfield shift at 151.29ppm. The chemical shift values of other carbon atoms of APE are observed at 130.81, 127.75 and 113.70 ppm and are attributed to C4, C2 and C6, respectively. The methyl carbon atom (C9) connected to the O8 oxygen atom of APE give signal in the upfield chemical shift at 26.07 ppm. The ^{1}H chemical shifts of APE are obtained by complete analysis of their NMR spectra and interpreted critically in an attempt to quantify the possible different effects acting on the shielding constant and in turn to the chemical shift of protons. The hydrogen atom H13, H14, H18 and H19 attached with the aromatic carbons of APE shows three peaks at 7.80, 6.64and 6.63 and 7.78 ppm, respectively. The hydrogen atom H19, H20 and H21 attached with the methyl carbon of APE are in the same chemical environment and shows one peak at 2.49 ppm. The experimental ^{1}H and ^{13}C NMR chemical shifts are represented in the Fig.8

12. Fukui Function

Fukui indices are, in short, reactivity indices, they give us information about which atoms in a molecule have a larger tendency to either loose or accept an electron, which we chemist interpret as which are more prone to undergo a

nuclophilic or an electrophilic attack, respectively. The fukui function is defined by R.G Parr [46] as $F(r) = (\delta\rho(r)/\delta(N))r$

Where δ(r) is the electronic density, N is the number of electrons and r is the external potential exerted by the nuclease. fukui function(FF) is the one of the widely used local density functional descriptors to model chemical reactivity and selectivity. The fukui function is a local reactivity descriptors that indicates the preferred where a chemical species will change its density when the number of electron is modified. Therefore, it indicates the propensity of the electronic density to perform at a given position upon accepting or donating electron [47-48]. Also, it is possible to define the corresponding condensed or atomic Fukui functions on the j th atom site as,

$$F_j^+ = q_j(N+1) - q_j(N)$$
$$F_j^- = q_j(N) - q_j(N-1)$$
$$F_j^0 = \tfrac{1}{2}[q_j(N+1) - q_j(N-1)]$$

Where f^k_j and f^-_j describe the ability of an atom to accommodate an extra electron or to cope with lose of an electron and f_j^o is then considered as an indicator for radical reactivity on the reference molecule. In these equation, q_j is the atomic charge (evaluated from mulliken population, electrostatic derived charges, etc) at the j^{th} atomic site is the neutral (N), anionic (N+1) or cationic (N-1)chemical species. P.K Chattaraj [49] have introduced the concept of generalized philicity. It contains almost all information about hitherto known different global and local reactivity and selectivity descriptor, in addition to the information regarding electrophilic / nucleophilic power of a given atomic site in a molecule. Morel c et al., [50] have recently proposed a dual descriptor (Δf(r)), which is defined as the difference between the nucleophilic and electrophilic fukui fuction and is given by the equation,

$$\Delta f(r) = [f^+(r) - f^-(r)]$$

Δf(r)>0, then the site is favored for a nucleophilic attack, whereas if Δf(r)<0, then the site may be favored for an electrophilic attack. According to dual descriptor Δf(r) provide a clear difference between nucleophilic and electrophilic attack at a particular site with their sign. That is they provide positive value for sited prone for nucliophilic attack and a negative value prone for electrophilic attack. From the values reported in Table.11. according to the condition for dual descriptor, nucleophilic sit for in our title molecule is C1, C5, O8, C9, H11, H13, N15 (positive value i.e. Δf(r) >0).Similarly the electrophilic site is C2, C4, C6, C7, H10, H12, H14, H16, H17, H18, H18 (Negative i.e. Δf (r)<0).The behavior of molecule as electrophilic and nucliophilic attack during reaction depends on the local behavior of molecule.

13. Thermodynamic Properties

For the title compound, the standard thermodynamic functions: heat capacity($C^0_{p:m}$), entropy (S^0_m) and enthalpy (H^0m), Gibb's free energy (G^0_m) were calculated based on the vibrational analysis by B3LYP method with cc-pVDZ and cc-pVTZ basis sets and statistical thermodynamics were obtained and listed in Table 12. It is noted from Table 12 that the standard heat capacities, entropies and enthalpies increase from 10 to 200 K, because the intensities of molecular vibration increase with the increasing temperature. According to the data in Table 12 for the title compound, the corresponding relations between the thermodynamic properties heat capacity, entropies, enthalpies and temperature are described and shown in fig.9.

14. Conclusions

The FT-IR, FT-Raman and NMR spectral studies and quantum chemical parameters, magnetic susceptibility of APE were carried out for the first time. Complete vibrational and molecular structure analyses have been performed based on the quantum mechanical approach by DFT calculations. The differences between the observed and scaled wavenumber values of the most of the fundamentals are very small. Therefore, the assignments made at DFT levels of theory with only reasonable deviations from the experimental values seem to be correct. The NBO result reflects the charge transfer mainly due to NH_2 and CH_3 groups. The dipole moment, polarizability and first order hyperpolarizabilities reveal that APE behave as interesting NLO materials. The lowering of HOMO–LUMO band gap supports bioactive property of the molecule. Furthermore, information about the size, shape, charge density distribution and site of chemical reactivity of the molecule has been obtained by mapping electron density isosurface with MESP and Fukui fuctions. Therefore, the results presented in this work for APE molecule indicates that these level of theory are reliable for prediction of both infrared and Raman spectra of the title molecule.

15. Acknowledgement

The authors acknowledge SAIF-IIT Madras, Chennai for spectral measurement and one of the authors M.Karunanidhi acknowledges the UGC, Ministry of HRD, Govt. of India, for assistance in the form of Minor Research Project.[UGC-SERO-NO.F.MRP-6116/15].

References

[1] M. Sittig, Handbook of Toxic and Hazardous Chemicals and Carcinogens, second ed., Noyes Publications, Park Ridge, NJ, 1985.
[2] R. Stewart, K. Yates, J. Am. Chem. Soc. 80 (1958) 6355.
[3] S. Forsen, B. Akermark, T. Alm, Acta Chem. Scand. 18 (1964) 2313–2328nt,
[4] Fu, H.B.;Yao, J.N.Size Effects on the optical properties of Organic Nanoparticles. J.Am. Chem. Soc.2001, 123, 1434- 1439.
[5] M.K. Subramanian, P.M. Anbarasan, V. Ilangovan, S. Moorthy Babu, Spectrochim.Acta A 71 (2008) 59–67.
[6] S.K. Seth, D.K. Hazra, Monika Mukherjee, Tanusree Kar, J. Mol. Struct. 936 (2009)277–282.
[7] K. Pei, Y. Ma, X. Zheng, H. Li, Chem. Phys. Lett. 437 (2007) 153–158.
[8] M. Frisch, G.W. Trucks, H.B. Schlegal, G.E. Scuseria, M.A. Robb, J.R. Cheesman,V.G. Zakrzewski, J.A. Montgomerg, Jr., R.E. Strtmann, J.C. Burant, S. Dapprich, J.M.Milliam, A.D. Daniels, K.N. Kudin, M.C. Strain, O. Farkas, J. Tomasi, V. Barone,M. Cossi, R. Camme, B. Mennucci, C. Pomelli, C. Adamo, S. Clifford, J. Ochterski,G.A. Petersson, P.Y. Ayala, Q.

Cui, K. Morokuma, N. Rega, P. Salvador, J.J.Dannenberg, D.K. Malich, A.D. Rabuck, K. Raghavachari, J.B. Foresman, J.Cioslowski, J.V. Ortiz, A.G. Baboul, B.B. Stetanov, G. Liu, A. Liashenko, P. Piskorz,I. Komaromi, R. Gomperts, R.L. Martin, D.J. Fox, T. Keith, M.A. Al-Laham, C.Y.Peng, A. Nsnsyskkara, M. Challacombe, P.M.W. Gill, B. Johnson, W. Chen, M.W.Wong, J.L. Andres, C. Gonzalez, M. Head-Gordon, E.S. Replogle, J.A. Pople,GAUSSIAN 09, Revision A.02, Gaussian, Inc, Pittsburgh, PA, 2009.

[9] A.D. Becke, J. Chem. Phys. 98 (1993) 5648.

[10] C. Lee, W. Yang, R.G. Parr, Phys. Rev. 37 (1998) 785.

[11] T. Sundius, J. Mol. Struct. 218 (1990) 321.

[12] T. Sundius, Vib. Spectrosc. 29 (2002) 89.

[13] M.J. Frisch, A.B. Nielson, A.J. Holder, Gaussview Users Manual, Gaussian Inc.,Pittsburgh, PA, 2000.

[14] P.L. Polavarapu, J. Phys.Chem. 94 (1990) 8106.

[15] G. Keresztury, S. Holly, J. Varga, G.A. Besenyei, Y. Wang, J.R. Durig, Spectrochim.Acta Part 49A (1993) 2007.

[16] G. Keresztury, Raman Spectroscopy: Theory in: J.M. Chalmers, P.R. Griffiths (Ed.), Hand book of Vibrational Spectroscopy, vol. 1, Wiley, 2002.

[17] G. Ma, B.O. Patrick, T.Q. Hu, B.R. James, Acta Cryst. E59 (2003) o579–o580.

[18] Y. Tanimoto, H. Kobayashi, S. Nagakura, Y. Saito, Acta Crystallogr. B29 (1973)1822–1826. (2004) 67–72.

[19] P.C. Chen, W. Lo, S.C. Tzeng, J. Mol. Struct. (Theochem.) 148 (1998) 257–266.

[20] P.C. Chen, W. Lo, K.H. Hu, Theor. Chem. Acta 95 (1997) 99–112.

[21] P.C. Chen, Y.C. Chieh, J. Mol. Struct. (Theochem.) 583 (2002) 173–180.

[22] G. Varsanyi, Assignments for Vibrational Spectra of Seven Hundred Benzene Derivatives, vol. 1, Adam Hilger, London, 1974.

[23] L.J. Bellamy, The Infrared Spectra of Complex Molecules, third ed., Wiley, NewYork, 1975.

[24] N. Misra, O. Prasad, L. Sinha, A. Pandey, J. Mol. Struct.: (Theochem.) 822 (2007)45–47.

[25] V. Arjunan, S. Thillai Govindaraja, S. Subramanian, S. Mohan, J. Mol. Struct. 1037 (2013) 73–84.

[26] D. Sajan, I. Hubert Joe, V.S. Jayakumar, J. Raman Spectrosc. 37 (2005) 508–519.

[27] P.S. Kalsi, Spectroscopy of Organic Compounds, Wiley Eastern Limited, New Delhi, 1993, pp. 117–118.

[28] A.R. Prabakaran, S. Mohan, Indian J. Phys. 63B (1989) 468–473.

[29] T. Kolev, J. Mol. Struct. 349 (1995) 381–384.

[30] G. Socrates, Infrared, Raman Characteristic Group Frequencies, Tables and Charts, third ed., Wiley, Chichester, 2001.

[31] R.N. Medhi, R. Barman, K.C. Medhi, S.S. Jois, Spectrochim. Acta 56A (2000)1523–1532.

[32] J.S. Murray, K. Sen, Molecular Electrostatic Potentials, Concepts and Applications, Elsevier, Amsterdam, 1996.

[33] I. Fleming, Frontier Orbitals and Organic Chemical Reactions, John Wiley andSons, New York, 1976. pp. 5–27.

[34] J.M. Seminario, Recent Developments and Applications of Modern Density Functional Theory, vol. 4, Elsevier, 1996. pp. 800–806.

[35] A.E. Reed, F. Weinhold, J. Chem. Phys. 83 (1985) 1736–1740.

[36] A.E. Reed, R.B. Weinstock, F. Weinhold, J. Chem. Phys. 83 (1985) 735–746.

[37] A.E. Reed, F. Weinhold, J. Chem. Phys. 78 (1983) 4066–4073.

[38] J.P. Foster, F. Weinhold, J. Am. Chem. Soc. 102 (1980) 7211–7218.

[39] M.C.Gupta, Atomic and Molecular Spectroscopy, New Age International Private Limited, Publishers, New Delhi, 2001.

[40] P.V.R. Schleyer, N.L. Allinger, T. Clark, J. Gasteiger, P.A. Kolmann, H.F. Schaefer, P.R. Schreiner, The Encyclopedia of Computational Chemistry, John Wiley &Sons, Chichester, 1998.

[41] R. Ditchfield, Mol. Phys. 27 (1974) 789–807.

[42] M. Barfiled, P. Fagerness, J. Am. Chem. Soc. 119 (1977) 8699–8711.

[43] J.M. Manaj, D. Maciewska, I. Waver, Magn. Reson. Chem. 38 (2000) 482– 485.

[44] A.J.D. Melinda, Solid State NMR Spectroscopy; Principles and Applications, Cambridge Press, 2003.

[45] R.M. Silverstein, F.X. Webster, Spectrometric Identification of Organic Compounds, sixth ed., John Wiley & Sons, Chichester, 2004.

[46] R.G.Parr, W.Yang, Densitynfunctional Theory of Atoms and Molecules, Oxford University Press, New York, 1989.

[47] P.W.Ayers, R.G.Parr, j. Am. Chem. Soc, 122 (2000) 2010-2018.

[48] R.G.Parr, W.Yang, j. Am. Chem. Soc, 106 (1984) 511-516.

[49] P.K.Chattaraj, B.Maiti, U.Sarkar, j. Phys. Chem. A 107(2003) 4973-4975.

[50] C.Morell, A.Grand, A.Toro-Labbe, J.Phys.Chem. A (2005)205-212.

Table 1: Optimized structural parameters of 1(4-Aminophenyl)ethanone utilizing B3LYP/cc-pVDZ and B3LYP/cc-pVTZ density functional calculation

Parameters	Bond length (A^0)		Parameters	Bond angle (A°)		Parameters	Dihedral angle (A°)	
	B3LYP/ cc-pVDZ	B3LYP/ cc-pVTZ		B3LYP /cc-pVDZ	B3LYP/ cc-pVTZ		B3LYP/ cc-pVDZ	B3LYP/ cc-pVTZ
C1-C2	1.407	1.399	C2-C1-C6	117.74	117.82	C6-C1-C2-C3	0	0.02
C1-C6	1.409	1.401	C2-C1-C7	123.67	123.28	C6-C1-C2-H13	180	179.92
C1-C7	1.489	1.485	C6-C1-C7	118.59	118.90	C7-C1-C2-C3	-180	-179.90
C2-C3	1.390	1.383	C1-C2-C3	121.39	121.33	C7-C1-C2-H13	0	0.01
C2-H13	1.092	1.081	C1-C2-H13	120.27	120.22	C2-C1-C6-C5	0	0.02
C3-C4	1.413	1.402	C3-C2-H13	118.35	118.46	C2-C1-C6-H19	-180	-179.91
C3-H14	1.093	1.083	C2-C3-C4	120.55	120.50	C7-C1-C6-C5	180	179.94
C4-C5	1.415	1.405	C2-C3-H14	120.01	120.00	C7-C1-C6- H19	0	0.01

C4-N15	1.370	1.381	C4-C3-H14	119.44	119.50	C2-C1-C7-O8	180	179.72
C5-C6	1.385	1.378	C3-C4-C5	118.26	118.43	C2-C1-C7-C9	0	-0.30
C5-H18	1.094	1.083	C3-C4-N15	120.94	120.85	C6-C1-C7-O8	0	-0.20
C6-H19	1.091	1.081	C5-C4-N15	120.80	120.67	C6-C1-C7-C9	180	179.79
C7-O8	1.224	1.218	C4-C5-C6	120.50	120.53	C1-C2-C3-C4	0	-0.01
C7-C9	1.522	1.518	C4-C5-H18	119.35	119.38	C1-C2-C3-H14	-180	-179.78
C9-H10	1.103	1.092	C6-C5-H18	120.15	120.09	H13-C2-C3-C4	-180	-179.92
C9-H11	1.103	1.092	C1-C6-C5	121.56	121.39	H13-C2-C3-H14	0	0.31
C9-H12	1.097	1.086	C1-C6-H19	117.77	118.05	C2-C3-C4-C5	0	-0.04
N15-H16	1.009	1.006	C5-C6-H19	120.67	120.56	C2-C3-C4-N15	-180	-177.50
N15-H17	1.009	1.006	C1-C7-O8	121.09	121.17	H14-C3-C4-C5	180	179.74
			C1-C7-C9	118.75	118.84	H14-C3-C4-N15	0	2.27
			O8-C7-C9	120.16	119.99	C3-C4-C5-C6	0	0.07
			C7-C9-H10	111.07	111.09	C3-C4-C5-H18	-180	-179.76
			C7-C9-H11	111.07	111.11	N15-C4-C5-C6	180	177.54
			C7-C9-H12	108.69	108.58	N15-C4-C5-H18	0	-2.29
			H10-C9-H11	107.26	107.38	C3-C4-N15-H16	0	-21.60
			H10-C9-H12	109.37	109.33	C3-C4-N15-H17	-180	-161.19
			H11-C9-H12	109.37	109.33	C5-C4-N15-H16	180	161.00
			C4-N15-H16	121.01	116.97	C5-C4-N15-H17	0	21.41
			C4-N15-H17	120.88	116.86	C4-C5-C6-C1	0	-0.07
			H16-N15-H17	118.11	113.61	C4-C5-C6-H19	180	179.86
						H18-C5-C6-C1	180	179.76
						H18-C5-C6-H19	0	-0.31
						C1-C7-C9-H10	-60	-59.67
						C1-C7-C9-H11	60	59.80
						C1-C7-C9-H12	-180	-179.93
						O8-C7-C9-H10	120	120.31
						O8-C7-C9-H11	-120	-120.21
						O8-C7-C9-H12	0	0.05

Table 2: Experimental FT-IR, FT-Raman and Calculated DFT-B3LYP/cc-pVDZ, B3LYP/cc-pVTZ levels of vibrational frequencies, IR intensity and Raman intensity of 1(4-Aminophenyl)ethanone

No	Spe.	Observed frequencies (cm^{-1})		Calculated frequencies (cm^{-1})				IR Intensity ($kmmol^{-1}$)		Raman Intensity ($kmmol^{-1}$)		Vibrational assignments /PED (≥ 10%)
				B3LYP/cc-pVDZ		B3LYP/cc-pVTZ						
		IR	Raman	Unscaled	Scaled	Unscaled	Scaled	B3LYP/cc-pVDZ	B3LYP/cc-pVTZ	B3LYP/cc-pVDZ	B3LYP/cc-pVTZ	
1	A'	3395s		3738	3398	3680	3394	32.2198	19.48	4.97	7.78	ν ass NH_2(98)
2	A'	3329vs	3325s	3610	3341	3577	3330	32.220	45.22	18.88	33.26	ν ss NH_2(96)
3	A'	3086m		3209	3089	3199	3084	100.672	3.52	9.19	14.53	νCH(96)
4	A'	3063m	3065s	3196	3076	3190	3063	3.352	9.06	10.11	14.81	νCH(98)
5	A'		3046m	3165	3048	3160	3045	10.549	19.22	11.23	16.15	νCH(97)
6	A'		3025w	3165	3036	3160	3026	23.073	11.83	10.82	16.18	νCH(98)
7	A'		2975w	3152	2975	3141	2973	13.511	14.22	11.50	17.01	ν_{ass} CH_3(98)
8	A'	2842vw		3103	2843	3089	2840	13.848	9.85	5.86	8.30	ν assCH_3(97)
9	A'	2819w		3035	2824	3035	2820	10.267	3.84	17.78	30.41	νssCH_3(96)
10	A'	1647s	1650vs	1753	1659	1737	1653	3.836	183.23	36.52	60.99	νCO(76), δCC(18)
11	A'		1612w	1665	1618	1662	1610	171.873	284.33	100.00	81.90	νCC(71), δCH(19)
12	A"		1594vs	1625	1604	1646	1593	502.076	136.94	0.17	100.00	ρNH_2(88)
13	A'	1565m	1564vs	1608	1589	1607	1561	51.669	22.61	2.85	5.86	νCC(76), δCH(18)
14	A'	1514m	1516s	1548	1520	1551	1515	18.177	13.23	16.22	15.52	δCH(78), νCN(12)
15	A'	1437vs	1441m	1473	1448	1484	1440	6.765	8.82	2.36	8.79	δCH(76), νCC(18)
16	A'		1386w	1452	1389	1474	1382	19.907	15.74	11.80	5.15	δad CH_3(94)
17	A'		1375w	1441	1378	1473	1374	7.383	16.57	5.15	4.80	δad CH_3(93)
18	A'	1360vs		1376	1370	1389	1362	8.339	56.71	2.85	1.42	ν CC(66), δCN(16), δadCH3(10)
19	A'	1304m	1305m	1369	1312	1366	1302	40.611	1.14	1.63	0.93	δsd CH_3(88)
20	A'			1349	1299	1339	1293	93.351	14.04	4.54	3.40	νCN(68), δ CH(20), νCN(10),
21	A'		1277vs	1318	1280	1325	1275	85.273	65.83	2.12	7.01	δCH(76), νCC(12)
22	A'			1295	1199	1290	1192	4.107	261.19	32.88	62.20	ν CC(72), δCH(21), δsd CH_3(12)
23	A'	1173s	1171s	1189	1177	1203	1170	219.709	108.85	6.53	18.49	δ CH(88)
24	A'	1134s		1138	1343	1156	1335	96.943	9.81	1.10	1.63	δ CH(85)
25	A"	1073w	1073s	1088	1079	1093	1074	15.399	2.99	23.92	53.32	σar CH_3(82), δring(12)

26	A'	1028w	1035w	1040	1038	1076	1029	1.480	1.48	0.28	1.98	σsr CH_3(89)
27	A'		1003w	1036	1009	1049	1004	1.314	0.61	1.25	0.05	σNH_2(78)
28	A"	958vs	960m	1015	975	1028	962	0.436	0.30	2.33	2.51	δring(71)
29	A"		943w	1000	958	1004	945	0.714	0.71	0.83	0.41	γCH(66),σar CH_3(27)
30	A"		901w	961	909	967	900	0.774	0.32	1.08	0.55	γCH(73)
31	A"	839vs	842s	953	851	956	945	0.363	49.04	15.19	21.46	ν CH_3(70),σsr CH_3(17)
32	A'		823m	850	835	853	820	44.009	36.45	55.66	19.29	δring(70)
33	A"		811w	844	827	846	812	2.456	9.53	2.26	74.23	γCH(71), δad CH_3(12)
34	A"		785w	819	793	826	783	26.705	8.15	6.80	2.15	γCH(82)
35	A"		733w	754	746	752	730	4.931	0.77	0.00	0.91	γ ring(78),γCC(10)
36	A'	697s	689m	699	706	698	695	0.075	2.25	8.81	12.12	δCO(68), δCC(18)
37	A"		636m	648	649	654	637	0.537	1.02	13.45	20.15	γ ring(67)
38	A"	596s		605	603	602	591	1.127	11.78	1.59	1.28	γCO(55),γCC(18),γCH(10)
39	A'	560s	564m	576	569	579	560	12.055	15.53	4.64	8.14	δring(62), δCO(21)
40	A"		496w	510	508	517	495	30.740	73.93	0.59	19.22	γ ring(57),γCN(12),γCO(10)
41	A'		436w	469	443	476	435	9.469	239.24	5.70	63.90	νCC(70), δCH(21)
42	A'		405w	427	419	469	408	2.335	106.74	0.65	12.15	νCC(71), δCH(19)
43	A'		388w	417	401	424	388	0.000	0.11	3.95	0.04	τNH_2(71)
44	A'		353m	379	363	385	350	0.004	1.39	3.81	5.13	δCN(68)
45	A"		335w	340	349	355	332	2.361	13.70	24.84	4.22	γ ring(61),γCC(18)
46	A'		270w	278	282	340	275	0.146	0.94	6.81	32.18	δCC(69)
47	A"		185	193	198	277	188	2.051	4.29	4.73	13.00	γ CC(52)
48	A'			167	161	194	145	4.058	4.59	0.30	6.47	τCH_3(75)
49	A"		110s	105	106	149	100	0.257	0.09	50.94	0.09	γCN(62),γ CC(21)
50	A"		85m	83	89	104	84	0.618	0.70	101.18	58.73	γ CH_3(60),γ ring(61)
51	A'			37	36	73	33	3.411	3.65	293.00	111.76	δrockNH_2(79)

ν-stretching, δ -in-plane bending, γ-out-of-plane bending, ρ-scissoring, σ-rocking, τ-twisting, δring-in-plane bending ring, γring-out-of -plane bending ring .

Table 3: Accumulation of natural charges and electron population of atoms in core, valance, Rydberg orbitals of 1(4-Aminophenyl)ethanone

Atoms[a]	Charge (e)	Natural population (e)			Total (e)	Atoms[b]	Charge(e)	Natural population (e)			Total (e)
		Core	Valence	Rydberg				Core	Valence	Rydberg	
C4	0.209	1.999	3.775	0.017	5.791	C1	-0.187	1.999	4.171	0.017	6.187
C7	0.591	1.999	3.364	0.046	5.409	C2	-0.184	1.999	4.172	0.013	6.184
H10	0.229	0.000	0.768	0.003	0.771	C3	-0.270	1.999	4.256	0.014	6.270
H11	0.229	0.000	0.768	0.003	0.771	C5	-0.267	1.999	4.254	0.014	6.267
H12	0.237	0.000	0.759	0.004	0.763	C6	-0.158	1.999	4.142	0.017	6.158
H13	0.226	0.000	0.772	0.003	0.774	O8	-0.567	2.000	6.558	0.009	8.567
H14	0.221	0.000	0.776	0.003	0.779	C9	-0.716	1.999	4.709	0.008	6.716
H16	0.393	0.000	0.603	0.004	0.607	N15	-0.842	2.000	5.833	0.010	7.842
H17	0.394	0.000	0.602	0.004	0.606						
H18	0.222	0.000	0.775	0.003	0.778						
H19	0.240	0.000	0.755	0.005	0.760						

[a] Atoms containing positive charges [b] Atoms containing negative charges

Table 4 : Significant second-order interaction energy (E (2), kcal/mol) between donor and acceptor orbital of 1(4-Aminophenyl) ethanone calculated at B3LYP/cc-pVDZ level of theory.

Donor (i)	Acceptor (j)	E(2)[a] kcal/mol	$(\varepsilon_i - \varepsilon_j)$[b] a.u	F_{ij}[c] a.u	Donor (i)	Acceptor (j)	E(2)[a] kcal/mol	$(\varepsilon_i - \varepsilon_j)$[b] a.u	F_{ij}[c] a.u
σ(C1 - C2)	σ*(C1 - C6)	4.29	1.3	0.067	σ(C4 - N15)	σ*(C5 - C6)	2.06	1.34	0.047
σ(C1 - C2)	σ*(C2 - C3)	3.18	1.29	0.057	σ(C5 - C6)	σ*(C1 - C6)	3.21	1.29	0.057
σ(C1 - C2)	σ*(C3 - H14)	2.66	1.17	0.05	σ(C5 - C6)	σ*(C1 - C7)	3.86	1.1	0.059
σ(C1 - C2)	σ*(C6 - H19)	2.48	1.19	0.049	σ(C5 - C6)	σ*(C4 - C5)	3.18	1.28	0.057
σ(C1- C6)	σ*(C1 - C2)	4.32	1.29	0.067	σ(C5 - C6)	σ*(C4 - N15)	4.63	1.03	0.062
σ(C1 - C6)	σ*(C1 - C7)	2	1.1	0.042	σ(C5 - H18)	σ*(C1 - C6)	3.9	1.13	0.059
σ(C1 - C6)	σ*(C2 - H13)	2.77	1.17	0.051	σ(C5 - H18)	σ*(C3 - C4)	4.77	1.12	0.065
σ(C1 - C6)	σ*(C5 - C6)	2.79	1.29	0.054	σ(C6 - H19)	σ*(C1 - C2)	4.97	1.12	0.067
σ(C1 - C6)	σ*(C5 - H18)	2.68	1.17	0.05	σ(C6 - H19)	σ*(C4 - C5)	4.18	1.11	0.061
σ(C1 - C7)	σ*(C1 - C6)	2	1.22	0.044	σ(C7 - C9)	σ*(C1 - C6)	2.65	1.22	0.051

σ(C1 - C7)	σ*(C2 - C3)	2.79	1.22	0.052	σ(C9 - H10)	σ*(C7 - O8)	4.26	0.54	0.044
σ(C1 - C7)	σ*(C5 - C6)	2.81	1.21	0.052	σ(C9 - H11)	σ*(C7- O8)	4.26	0.54	0.044
σ(C2 - C3)	σ*(C1 - C2)	3.55	1.29	0.061	σ(C9 - H12)	σ*(C1 - C7)	3.81	0.92	0.054
σ(C2 - C3)	σ*(C1 - C7)	3.88	1.11	0.059	σ(N15 -H16)	σ*(C4 - C5)	2.94	1.26	0.054
σ(C2 - C3)	σ*(C3 - C4)	3.24	1.28	0.058	σ(N15 - H17)	σ*(C3 - C4)	2.95	1.25	0.055
σ(C2 - C3)	σ*(C4 - N15)	4.54	1.04	0.061	Lp σ(O8)	σ*(C1 - C7)	2.24	1.08	0.044
σ(C2 - H13)	σ*(C1 - C6)	4.66	1.13	0.065	Lp σ(N15)	σ*(C3 - C4)	28.59	0.28	0.085
σ(C2 - H13)	σ*(C3 - C4)	4.03	1.12	0.06	π(C7 - O8)	π*(C1- C2)	124.59	0.01	0.066
σ(C3 - C4)	σ*(C2 - C3)	2.98	1.31	0.056	π(C1 - C2)	π*(C3 - C4)	16.78	0.28	0.062
σ(C3 - C4)	σ*(C2 - H13)	2.51	1.19	0.049	π(C1 - C2)	π*(C5 - C6)	22.89	0.29	0.073
σ(C3 - C4)	σ*(C4 - C5)	4	1.3	0.064	π(C1 - C2)	π*(C7 - O8)	17.19	0.28	0.065
σ(C3 - C4)	σ*(C5 - H18)	2.51	1.19	0.049	π(C3 - C4)	π*(C1 - C2)	24.31	0.3	0.076
σ(C3 - H14)	σ*(C1 - C2)	3.98	1.13	0.06	π(C3 - C4)	π*(C5 - C5)	15.73	0.3	0.062
σ(C3 - H14)	σ*(C4 - C5)	4.71	1.12	0.065	π(C5 - C6)	π*(C1 - C2)	17.03	0.29	0.064
σ(C4 - C5)	σ*(C3 - C4)	4	1.3	0.064	π(C5 - C6)	π*(C3 - C4)	24.69	0.28	0.076
σ(C4 - C5)	σ*(C3 - H14)	2.53	1.19	0.049	π(C7 - O8)	π*(C1 - C2)	4.13	0.4	0.04
σ(C4 - C5)	σ*(C5 - C6)	2.85	1.3	0.055	π(O8)	π*(C1 - C7)	19.28	0.66	0.102
σ(C4 - C5)	σ*(C6 - H19)	2.29	1.21	0.047	π(O8)	π*(C7 - C9)	20.09	0.63	0.102
σ(C4 - N15)	σ*(C2 - C3)	2.08	1.34	0.047					

[a]E(2) means energy hyper conjugative interactions.
[b]Energy difference between donor and acceptor i and j NBO orbitals.
[c]F(i,j) is the Fock matrix element between i and j NBO orbitals.

Table 5: Natural atomic orbital occupancies and energies of most interacting NBO's of 1(4- Aminophenyl)ethanone along with their hybrid atomic orbitals and hybrid directionality.

Parameters[a] (A–B)	Occupancies	ED_A%	ED_B %	Energies(a.u)(A,B)	Hybrid	AO(%) [b]	%d
σ(C1-C2)	1.9735	50.41%	49.59%	0.710,0.704	$sp^{1.85}$(C1)$sp^{1.82}$(C2)	s(35.13%)+p(64.84%) s(35.46%)+p(64.50%)	0.00(0.03%) 0.00(0.03%)
σ(C1-C6)	1.9726	50.81%	49.19%	0.712,0.701	$sp^{1.83}$(C1)$sp^{1.82}$(C6)	s(35.33%)+p(64.64%) s(35.48%)+p(64.49%	0.00(0.03%) 0.00(0.04%)
σ(C1-C7)	1.9769	52.71%	47.29%	0.726,0.687	$sp^{2.39}$(C1)$sp^{1.85}$(C7)	s(29.52%)+p(70.45%) s(35.03%)+p(64.91%)	0.00(0.03%) 0.00(0.05%)
σ(C2-C3)	1.9733	49.98%	50.02%	0.706,0.707	$sp^{1.82}$(C2)$sp^{1.78}$(C3)	s(35.40%)+p(64.57%) s(36.02%)+p(63.95%)	0.00(0.03%) 0.00(0.03%)
σ(C2-H13)	1.9786	61.39%	38.61%	0.783,0.621	$sp^{2.44}$(C2)$sp^{0.00}$(H13)	s(29.04%)+p(70.94%) s(99.90%)+p(0.10%)	0.00(0.02%)
σ(C3-C4)	1.9739	49.36%	50.64%	0.702,0.711	$sp^{1.84}$(C3)$sp^{1.69}$(C4)	s(35.15%)+p(64.82%) s(37.13%)+p(62.83%)	0.00(0.04%) 0.00(0.03%)
σ(C3-H14)	1.9789	61.17%	38.83%	0.782,0.623	$sp^{2.48}$(C3)$sp^{0.00}$(H14)	s(28.73%)+p(71.25%) s(99.90%)+p(0.10%)	0.00(0.02%)
σ(C4-C5)	1.9743	50.74%	49.26%	0.712,0.701	$sp^{1.69}$(C4)$sp^{1.85}$(C5)	s(37.20%)+p(62.77%) s(35.07%)+p(64.89%)	0.00(0.03%) 0.00(0.04%)
σ(C4-N15)	1.9908	39.34%	60.66%	0.627,0.778	$sp^{2.93}$(C4)$sp^{1.62}$(N15)	s(25.39%)+p(74.51%) s(38.09%)+p(61.87%)	0.00(0.10%) 0.00(0.03%)
σ(C5-C6)	1.9735	50.29%	49.71%	0.709,0.705	$sp^{1.78}$(C5)$sp^{1.85}$(C6)	s(36.01%)+p(63.96%) s(35.07%)+p(64.90%)	0.00(0.03%) 0.00(0.03%)
σ(C5-H18)	1.9788	61.22%	38.78%	0.782,0.622	$sp^{2.47}$(C5)$sp^{0.00}$(H18)	s(28.81%)+p(71.18%) s(99.90%)+p(0.10%)	0.00(0.02%)
σ(C6-H19)	1.9785	62.28%	37.72%	0.789,0.614	$sp^{2.41}$(C6)$sp^{0.00}$(H19)	s(29.36%)+p(70.63%) s(99.89%)+p(0.11%)	0.00(0.02%)
σ(C7-O8)	1.9961	33.01%	66.99%	0.574,0.818	$sp^{2.28}$(C7)$sp^{1.30}$(O8)	s(30.41%)+p(69.38%) s(43.46%)+p(56.46%)	0.01(0.21%) 0.00(0.09%)
σ(C7-C9)	1.9886	48.24%	51.76%	0.6945.719	$sp^{1.91}$(C7)$sp^{2.72}$(C9)	s(34.37%)+p(65.58%) s(26.86%)+p(73.09%)	0.05%(0.05%)
σ(C9-H10)	1.9750	61.23%	38.77%	0.782,0.622	$sp^{3.14}$(C9)(H10)	s(24.13%)+p(75.85%) s(99.90%)+p(0.10%)	0.00(0.03%)
σ(C9-H11)	1.9750	61.23%	38.77%	0.782,0.622	$sp^{3.14}$(C9)$sp^{0.00}$(H11)	s(24.13%)+p(75.85%) s(99.90%)+p(0.10%)	0.00(0.03%)
σ(C9-H12)	1.9880	61.92%	38.08%	0.786,0.617	$sp^{3.03}$(C9)$sp^{0.00}$(H12)	s(24.82%)+p(75.16%) s(99.90%)+p(0.10%)	0.00(0.02%)
σ(N15-H16)	1.9938	69.87%	30.13%	0.835,0.548	$sp^{2.24}$(N15)$sp^{0.00}$(H16)	s(30.86%)+p(69.12%) s(99.77%)+p(0.23%)	0.00(0.03%)
σ(N15-H17)	1.9938	69.90%	30.10%	0.836,0.548	$sp^{2.24}$(N15)$sp^{0.00}$(H17)	s(30.89%)+p(69.08%) s(99.77%)+p(0.23%)	0.00(0.03%)
LP(O8)	1.9736				$sp^{0.77}$	s(56.52%)+p(43.46%)	0.00(0.02%)

LP(N15)	1.8319				$sp^{1.00}$	s(0.00%)+p(100.00%)	0.00(0.00%)
π (C3-C4)	1.6228	54.36%	45.64%	0.737,0.675	$sp^{1.00}$(C3)$sp^{1.00}$(C4)	s(0.00%)+p(99.95%) s(0.00%)+p(99.95%)	0.00(0.05%) 0.00(0.07%)
π (C5-C6)	1.6961	54.32%	45.68%	0.737,0.675	$sp^{1.00}$(C5)$sp^{1.00}$(C6)	s(0.00%)+p(99.93%) s(0.00%)+p(99.56%)	0.00(0.05%) 0.00(0.07%)
π (C7-O8)	1.9765	33.13%	66.87%	0.575,0.817	$sp^{1.00}$(C7)$sp^{1.00}$(O8)	s(0.00%)+p(99.86%) s(0.02%)+p(99.91%)	(0.44%) 0.00(0.14%)
LP (O8)	1.8832				sp99.99s	s(0.02%)+p(99.91%)	-0.07%
π (C1-C2)	1.6516	54.20%	45.80%	0.736,0.676	$sp^{1.00}$(C1)$sp^{1.00}$(C2)	s(0.00%)+p(99.97%) s(0.00%)+p(99.95%)	0.00(0.03%) 0.00(0.05%)

[a] For numbering of atoms refer Fig. 1
[b] Percentage of s-type and p-type subshell of an atomic orbitals are given in their respective brackets

Table 6: The DFT/ B3LYP/cc-pVDZ and B3LYP/cc-pVTZ level calculated electric dipole moments (Debye), Dipole moments compound, polarizability (in a.u), β components and β_{tot} (10^{-30} esu)value of (4-Aminophenyl)ethanone

Parameters	B3LYP/ cc-pVDZ	B3LYP/ cc-pVTZ	Parameters	B3LYP/ cc-pVDZ	B3LYP/ cc-pVTZ
μ_x	-4.7734	-4.2507	β_{xxx}	-88.5158	-71.7445
μ_y	2.3352	2.4531	β_{yyy}	-0.1571	0.5694
μ_z	0.0004	0.7748	β_{zzz}	0.0004	0.5409
μ	5.3139	4.9685	β_{xyy}	-17.427	-18.0187
α_{xx}	-47.8544	-52.0256	β_{xxy}	18.9802	20.4085
α_{yy}	-55.8095	-56.0645	β_{xxz}	0.0075	14.7055
α_{zz}	-61.6291	-62.0706	β_{xzz}	7.2819	7.0806
α_{xy}	6.7595	7.4095	β_{yzz}	-1.2067	-0.9237
α_{xz}	-0.0015	-3.5456	β_{YYZ}	0.0003	0.4766
α_{yz}	-0.0001	0.1352	β_{XYZ}	-0.0002	-0.3823
Δα(esu)	280.519388	279.114734	βtot(esu)	7.4832E-30	6.4602E-30

Table 7: Mulliken population analysis of 1(4-Aminophenyl)ethanone performed at B3LYP/cc-pVDZ and B3LYP/cc-pVTZ

Atoms	Atomic charges	
	B3LYP/cc-pVDZ	B3LYP/cc-pVTZ
C1	-0.561	-0.523
C2	0.206	0.175
C3	-0.248	-0.247
C4	0.683	0.658
C5	-0.224	-0.225
C6	0.184	0.159
C7	1.083	1.093
O8	-0.772	-0.791
C9	-0.105	-0.107
H10	0.003	0.007
H11	0.003	0.006
H12	0.006	0.011
H13	0.035	0.043
H14	0.008	0.019
N15	-0.786	-0.756
H16	0.203	0.192
H17	0.204	0.193
H18	0.007	0.018
H19	0.070	0.075

Table 8: Quantum Chemical Parameters of 1(4-Aminophenyl)ethanone calculated at B3LYP/cc-pVDZ and B3LYP/cc-pVTZ level of theory

Quantum Chemical Parameters	B3LYP/ CC-PVDZ	B3LYP/ CC-PVTZ
Ionisation potential(I)= (-Homo energy)	0.21354	0.22231
Electron Affinity(A)= (-Lumo Energy)	0.03892	0.04742
Homo-Lumo Energy gap	4.7515	4.7589
Hardness(η)=0.5*(I-A)	0.08731	0.087445
Electronegativity(X)=(I+A)/2	0.12623	0.134865
softness (σ) =1/η	11.45344	11.43576
Chemical potential(M) = -X	-0.12623	-0.13487
GlobalElectrophilicity(w) =(M*M)/(eta*2)	0.09125	0.104

Table 9: Magnetic susceptibility of 1(4-Aminophenyl)ethanone at various temperatures.

S.NO	Temp. (kelvin)	Susceptibility(χ_m) mole per m^3	1/susceptibility $1/(\chi_m)$
1	10	2.6418E-05	37852.98
2	20	1.3209E-05	75705.96
3	40	6.6045E-06	151411.9
4	60	4.403E-06	227117.9
5	80	3.3023E-06	302823.8
6	100	2.6418E-06	378529.8
7	120	2.2015E-06	454235.7
8	140	1.887E-06	529941.7
9	160	1.6511E-06	605647.7
10	180	1.4677E-06	681353.6
11	200	1.3209E-06	757059.6

Table 10: NMR Chemical shielding anisotropy (CSA) parameters of 1(4-Aminophenyl)ethanone

Proton	σ_{Tms}	B3lyp/ cc-pVDZ σ_{calc}	δcalc (σ_{Tms}-σ_{calc})	Exp δ_{ppm}	Carbon	σ_{Tms}	B3lyp/ cc-pVDZ σ_{calc}	δcalc (σ_{Tms}-σ_{calc})	Exp δ_{ppm}
H10	31.8821	29.5	2.3821	2.497	C1	182.46	31	151.46	151
H11	31.8821	29.5	2.3821	2.497	C2	182.46	54	128.46	127
H12	31.8821	29.8	2.0821	2.497	C3	182.46	68	114.46	113
H13	31.8821	24.1	7.7821	7.806	C4	182.46	52	130.46	130
H14	31.8821	25.4	6.4821	6.646	C5	182.46	70	112.46	113
H16	31.8821	27.5	4.3821	4.223	C6	182.46	55	127.46	127
H17	31.8821	27.6	4.2821	4.223	C7	182.46	-14.9	197.36	196
H18	31.8821	25.4	6.4821	6.630	C9	182.46	156	26.46	26
H19	31.8821	23.9	7.9821	7.789					

Table 11: Using Mulliken population analysis: Fukui's fuction (f_k^+,f_k^-,$f_k°$), Atomic softness, Electrophilicity of 1(4-Aminophenyl) ethanone

Mulliken atomic charges(a.u.)				Fukui's functions (a.u.)				Atomic softness			Electrophilicity indices		
Atoms	Neutral Atomic charges(N)	Cation (N-1)	Anion (N+1)	f_k^+	f_k^-	$f_k°$	Δf(r)	s_k^+	s_k^-	$s_k°$	ω_k^+	ω_k^-	$\omega_k°$
C1	-0.561	-0.459	-0.624	-0.063	-0.102	-0.083	0.039	-0.024	-0.039	-0.032	-0.206	-0.334	-0.270
C2	0.206	0.156	0.026	-0.180	0.050	-0.065	-0.230	-0.069	0.019	-0.025	-0.589	0.164	-0.213
C3	-0.248	-0.015	-0.136	0.112	-0.233	-0.061	0.345	0.043	-0.090	-0.023	0.366	-0.762	-0.198
C4	0.683	-0.103	-0.173	-0.856	0.786	-0.035	-1.642	-0.330	0.303	-0.013	-2.799	2.570	-0.114
C5	-0.224	0.214	0.028	0.252	-0.438	-0.093	0.690	0.097	-0.169	-0.036	0.824	-1.432	-0.304
C6	0.184	0.212	0.027	-0.157	-0.028	-0.093	-0.129	-0.060	-0.011	-0.036	-0.513	-0.092	-0.302
C7	1.083	-0.499	-0.666	-1.749	1.582	-0.084	-3.331	-0.674	0.609	-0.032	-5.719	5.173	-0.273
O8	-0.772	0.352	0.246	1.018	-1.124	-0.053	2.142	0.392	-0.433	-0.020	3.329	-3.675	-0.173
C9	-0.105	0.362	0.235	0.340	-0.467	-0.064	0.807	0.131	-0.180	-0.024	1.112	-1.527	-0.208
H10	0.003	0.159	-0.196	-0.199	-0.156	-0.178	-0.043	-0.077	-0.060	-0.068	-0.651	-0.510	-0.580
H11	0.003	0.831	0.737	0.734	-0.828	-0.047	1.562	0.283	-0.319	-0.018	2.400	-2.708	-0.154
H12	0.006	-0.019	-0.037	-0.043	0.025	-0.009	-0.068	-0.017	0.010	-0.003	-0.141	0.082	-0.029
H13	0.035	0.555	0.492	0.457	-0.520	-0.032	0.977	0.176	-0.200	-0.012	1.494	-1.700	-0.103
H14	0.008	-0.236	-0.301	-0.309	0.244	-0.033	-0.553	-0.119	0.094	-0.013	-1.010	0.798	-0.106
N15	-0.786	-0.257	-0.315	0.471	-0.529	-0.029	1.000	0.181	-0.204	-0.011	1.540	-1.730	-0.095
H16	0.203	-0.254	-0.314	-0.517	0.457	-0.030	-0.974	-0.199	0.176	-0.012	-1.691	1.494	-0.098
H17	0.204	-0.251	-0.313	-0.517	0.455	-0.031	-0.972	-0.199	0.175	-0.012	-1.691	1.488	-0.101
H18	0.007	-0.248	-0.312	-0.319	0.255	-0.032	-0.574	-0.123	0.098	-0.012	-1.043	0.834	-0.105
H19	0.07	-0.245	-0.311	-0.381	0.315	-0.033	-0.696	-0.147	0.121	-0.013	-1.246	1.030	-0.108

Table 12: Statistical thermodynamic parameters of 1(4-Aminophenyl)ethanone at various temperatures, performed at B3LYP/cc-pVDZ

Thermodynamic parameters (k cal mol^{-1})				
Temp. (Kelvin)	C_P	S	$(H^o - E^o_o)/T$	$(G_o - E^o_o)/T$
20	9.327	52.645	7.978	-44.667
40	11.619	59.102	8.310	-50.792
60	13.672	63.775	8.953	-54.822
80	15.570	67.808	9.820	-57.988
100	17.476	71.523	10.853	-60.670

120	19.441	75.058	12.015	-63.043
140	21.462	78.482	13.280	-65.202
160	23.525	81.837	14.633	-67.204
180	25.621	85.150	16.061	-69.089
200	27.743	88.437	17.555	-70.882

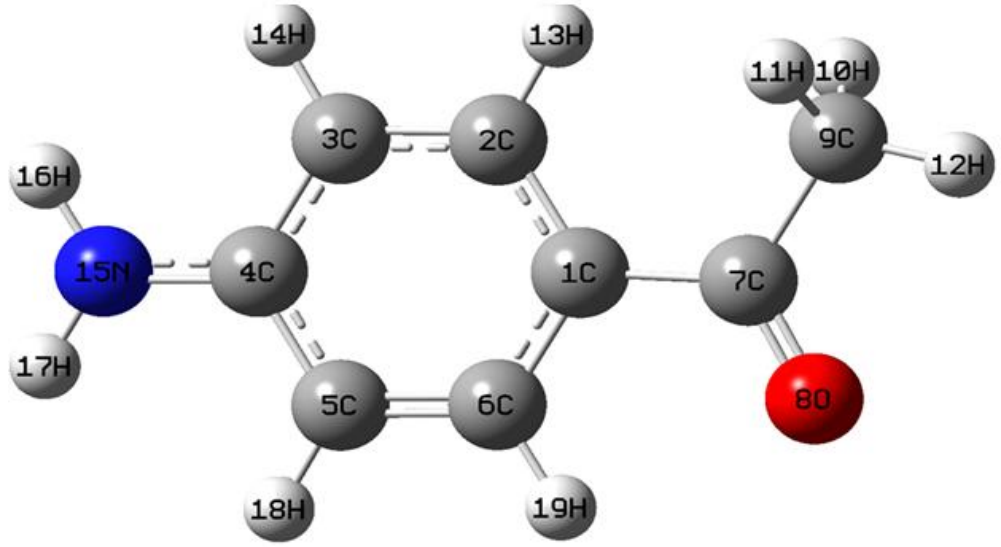

Figure 1: Optimized geometrical structure and atom numbering of 1(4-aminophenyl)ethanone

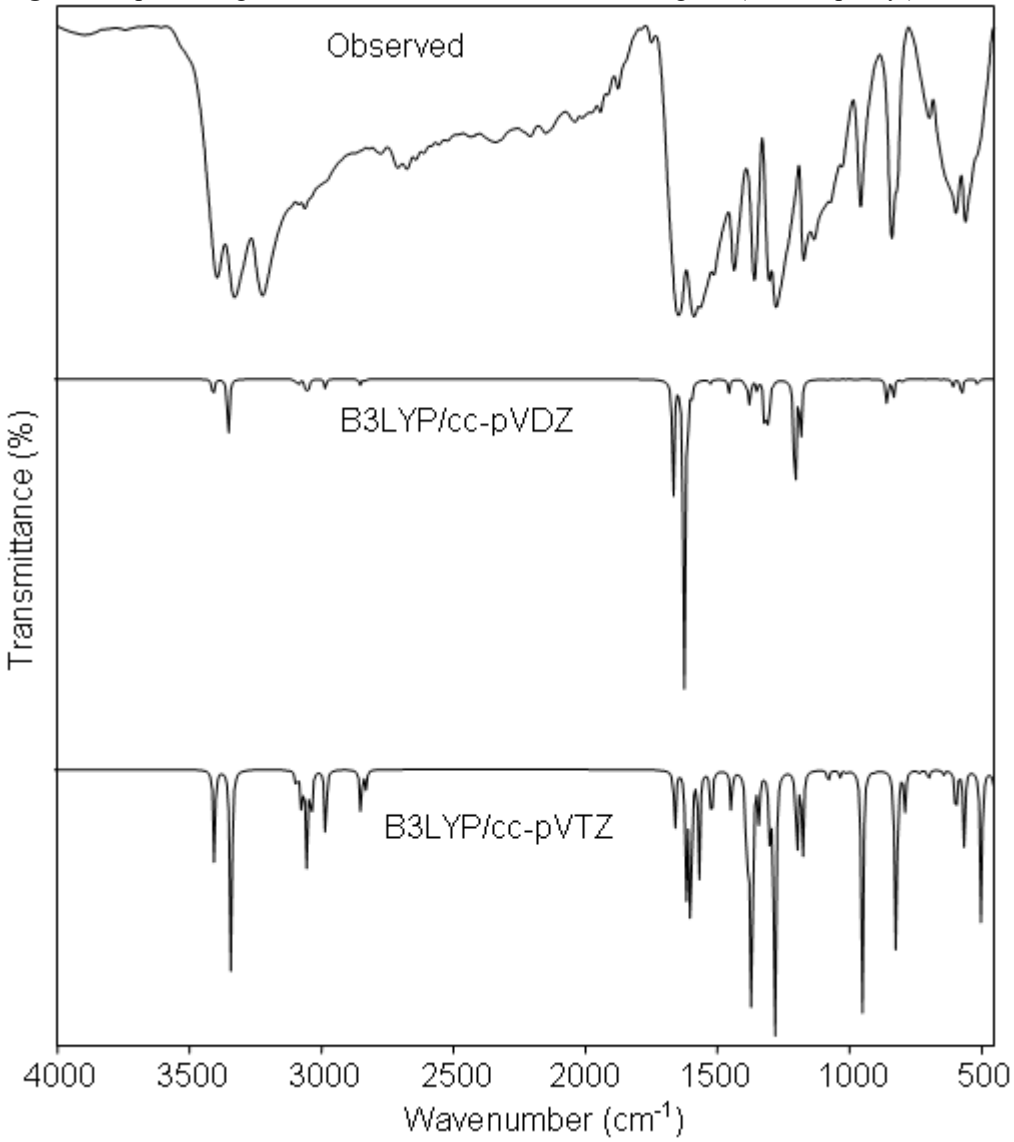

Figure 2: Observed and simulated infrared spectra of 1(4-aminophenyl)ethanone

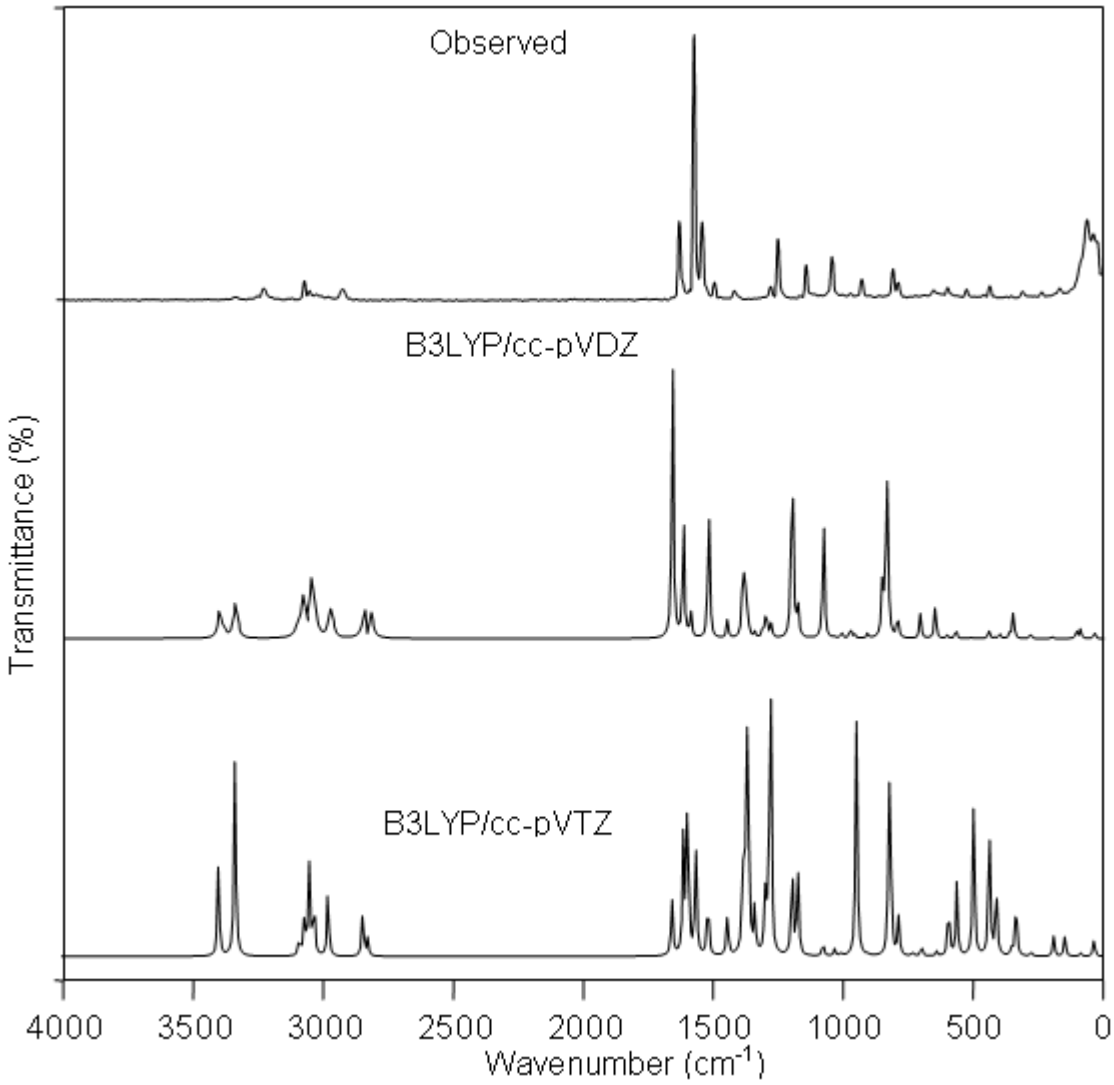

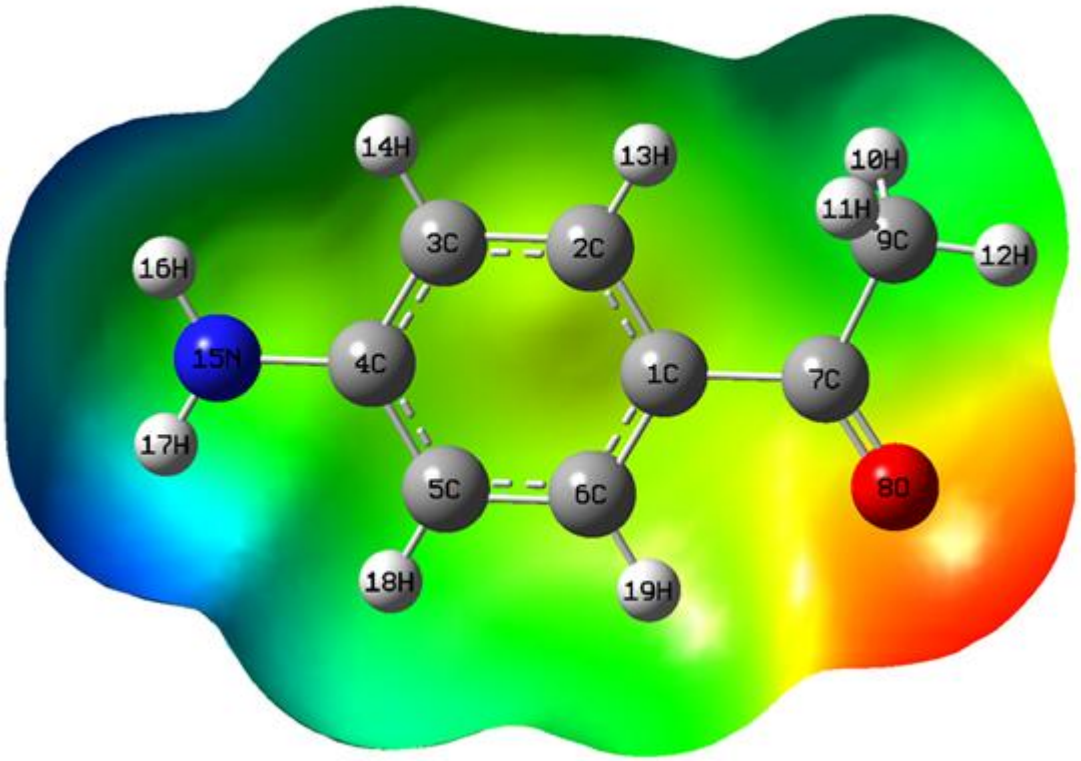

Figure 4 (a): Molecular Electrostatic Potential of 1(4-aminophenyl)eethanone

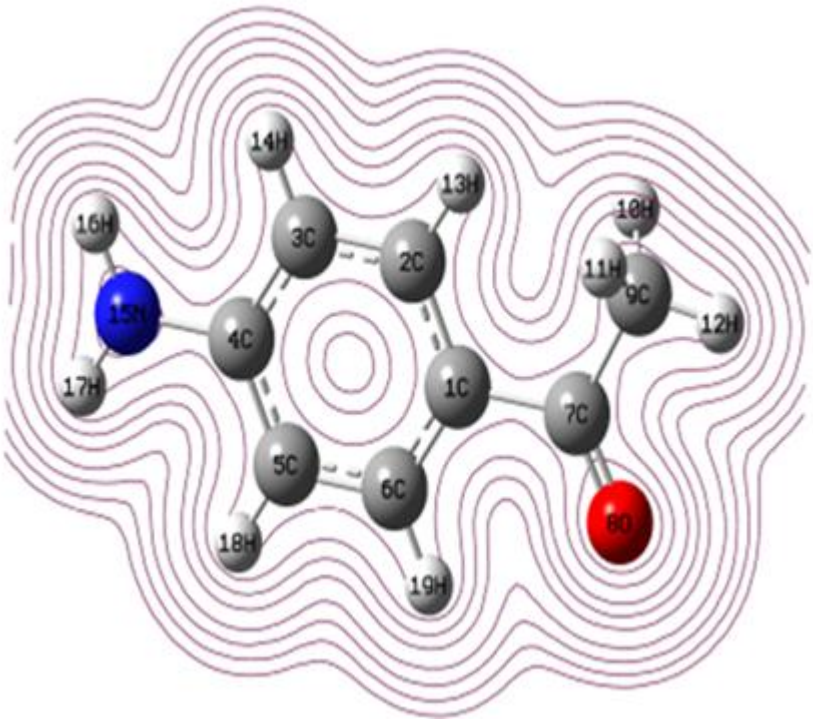

Figure 4 (b): Molecular electrostatic potential contour map of 1(4-aminophenyl)ethanone

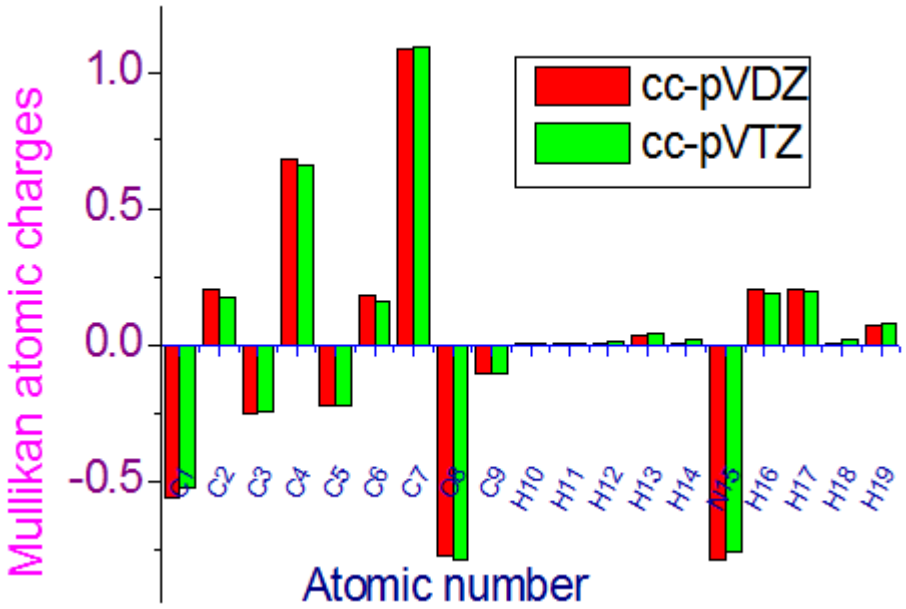

Figure 5: Mullikan atomic charges of 1(4-Aminophenyl)ethanone

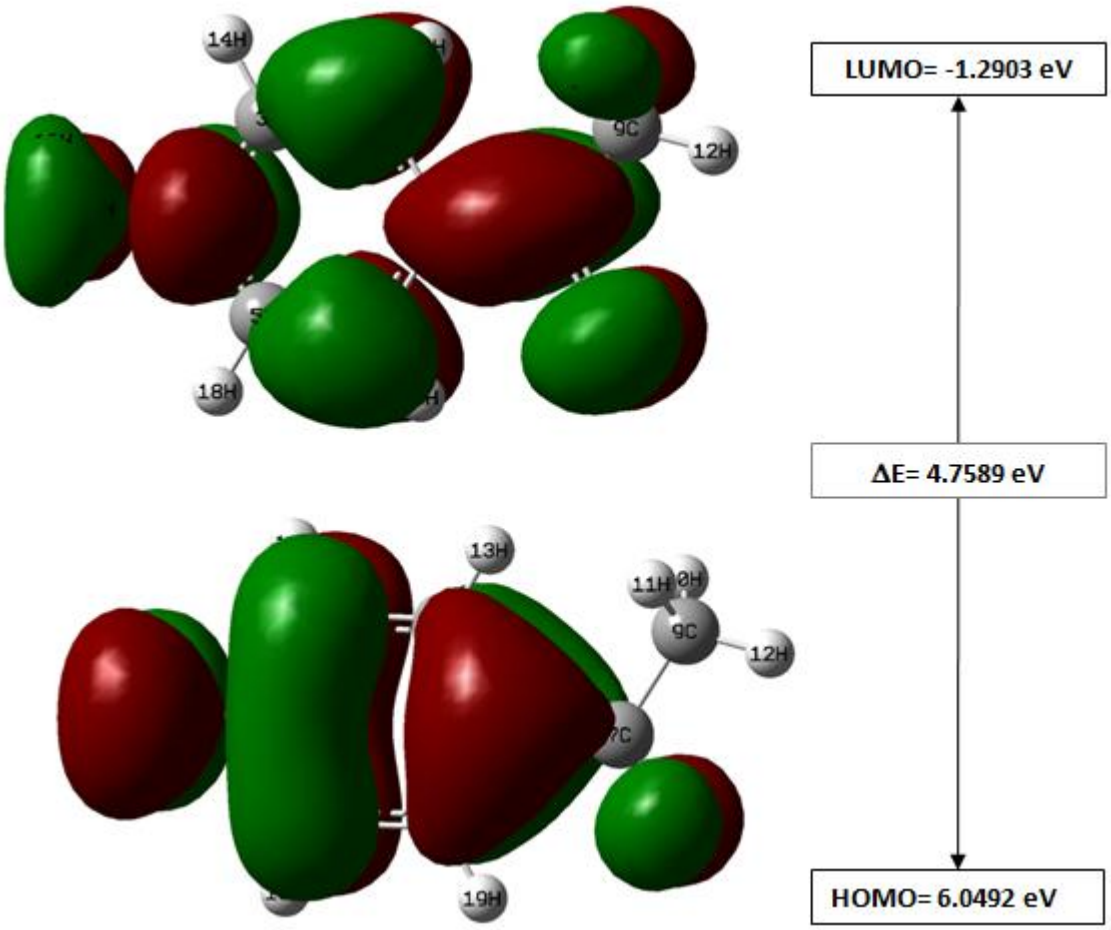

Figure 6: HOMO-LUMO plot of 1(4-aminophenyl)ethanone

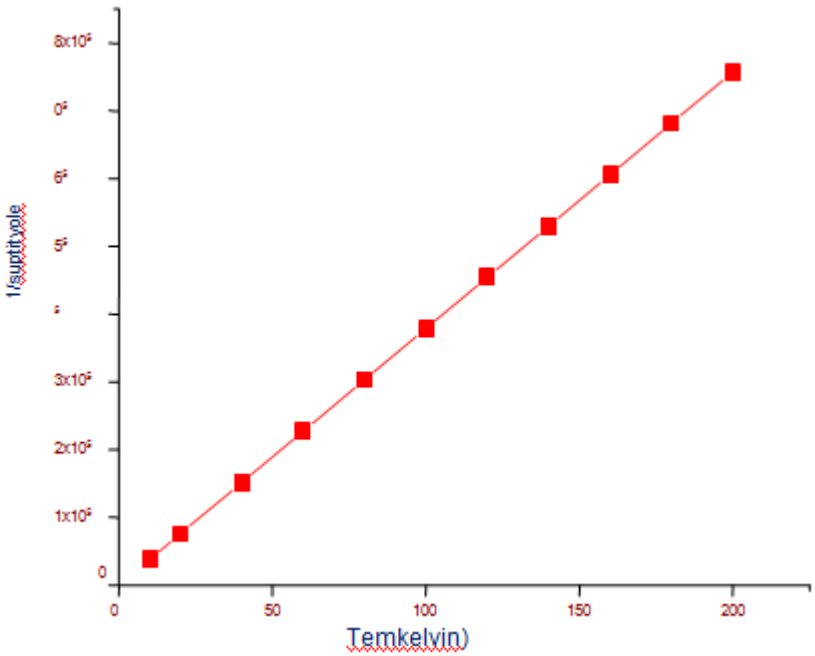

Figure 7: Magnetic susceptibility of 1(4-aminophenyl)ethanone

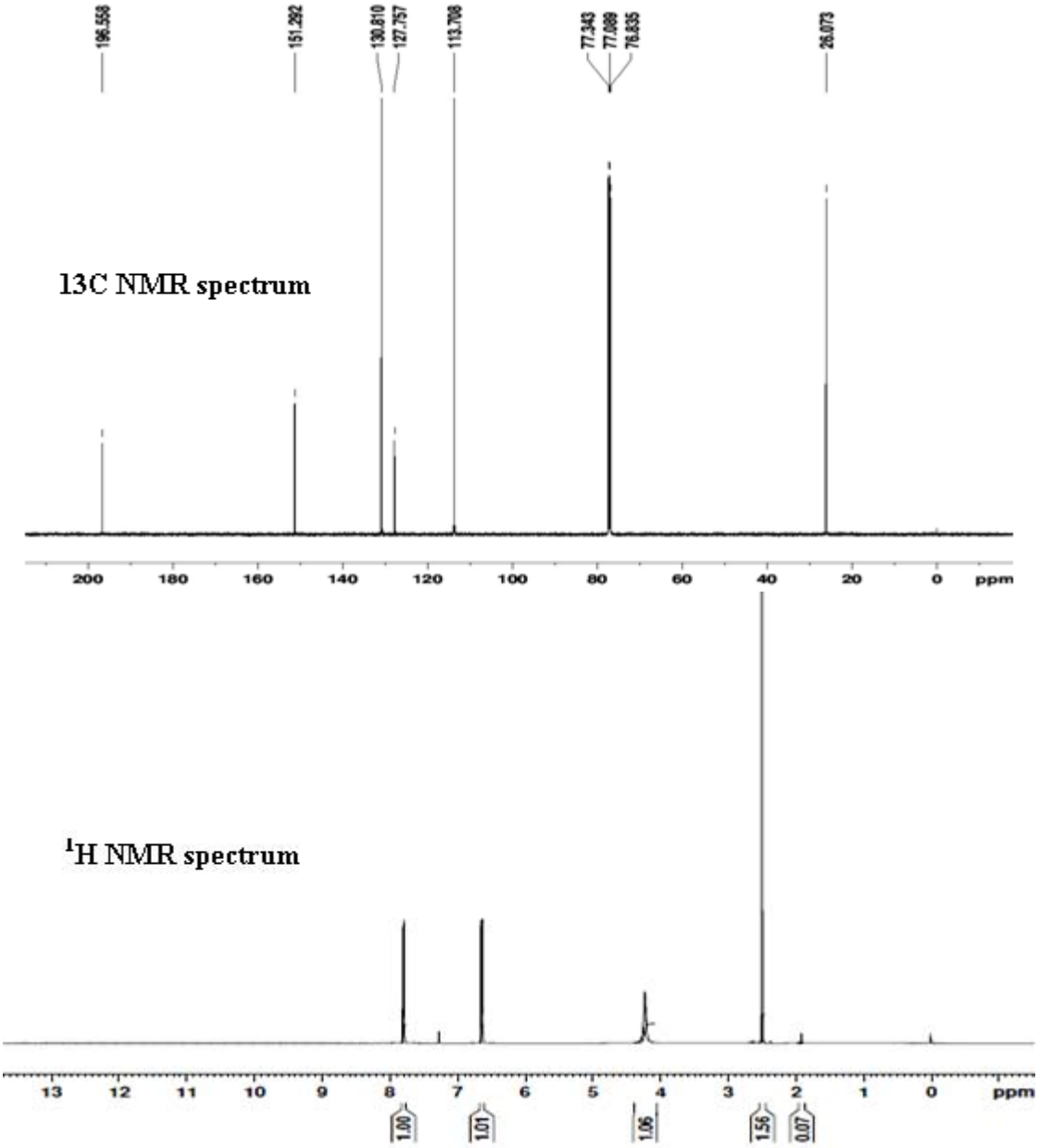

Figure 8: ^{13}C and ^{1}H NMR spectra of the of 1(4-aminophenyl)ethanone

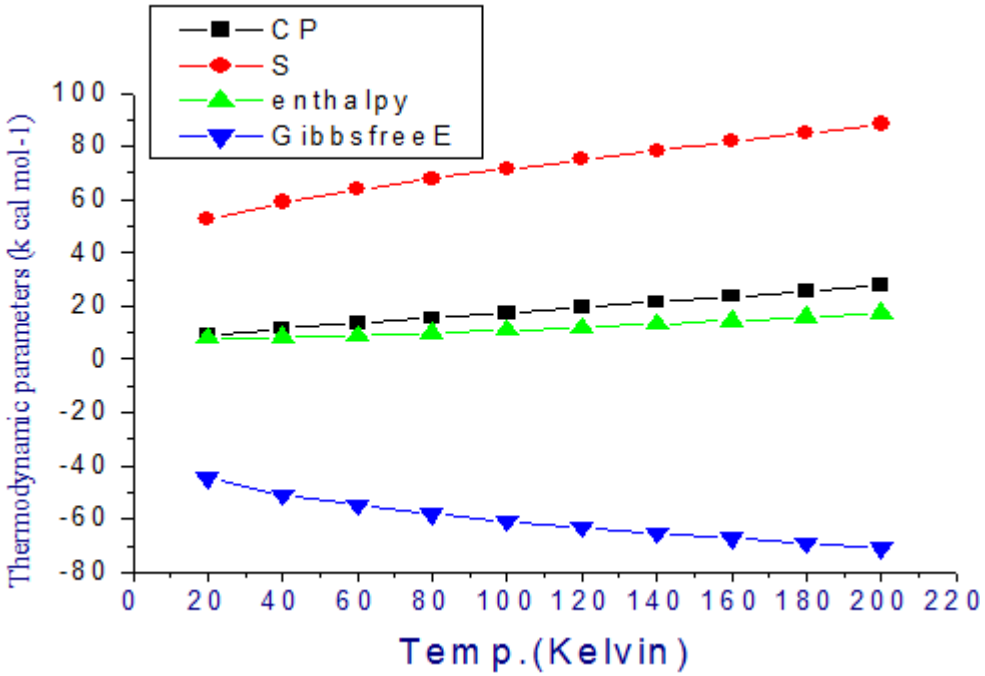

Figure 9: Thermodynamic properties of 1(4-aminophenyl)ethanone